JOURNAL OF VIROLOGY, June 1995, p. 3282–3289 Vol. 69, No. 6
0022-538X/95/$04.00+0

The Bovine Leukemia Virus Encapsidation Signal Is Discontinuous and Extends into the 5′ End of the *gag* Gene†

LOUIS M. MANSKY,* ANN E. KRUEGER, AND HOWARD M. TEMIN‡

McArdle Laboratory for Cancer Research, University of Wisconsin Medical School, Madison, Wisconsin 53706

Received 23 December 1994/Accepted 22 February 1995

In order to define bovine leukemia virus (BLV) sequences required for efficient vector replication, a series of mutations were made in a BLV vector. Testing the replication efficiency of the vectors with a helper virus and helper plasmids allowed for separation of the mutant vectors into three groups. The replication efficiency of the first group was reduced by a factor of 7; these mutants contained deletions in the 5′ end of the *gag* gene. The second group of mutants had replication reduced by a factor of 50 and had deletions including the 5′ untranslated leader region. The third group of mutants replicated at levels comparable to those of the parental vector and contained deletions of the 3′ end of the *gag* gene, the *pol* gene, and the *env* gene. Analysis of cytoplasmic and virion RNA levels indicated that vector RNA expression was not affected but that the vector RNA encapsidation was less efficient for group 1 and group 2 mutants. Additional mutations revealed two regions important for RNA encapsidation. The first region is a 132-nucleotide-base sequence within the *gag* gene (nucleotides 1015 to 1147 of the proviral DNA) and facilitates efficient RNA encapsidation in the presence of the second region. The second region includes a 147-nucleotide-base sequence downstream of the primer binding site (nucleotide 551) and near the *gag* gene start codon (nucleotide 698; *gag* begins at nucleotide 628) and is essential for RNA encapsidation. We conclude that the encapsidation signal is discontinuous; a primary signal, essential for RNA encapsidation, is largely in the untranslated leader region between the primer binding site and near the *gag* start codon. A secondary signal, which facilitates efficient RNA encapsidation, is in a 132-nucleotide-base region within the 5′ end of the *gag* gene.

Retroviral vectors have been useful for studying various aspects of retroviral replication and for many applications of gene transfer. A retroviral vector contains all the *cis*-acting sequences necessary for retrovirus replication but is deficient in the production of some or all of the viral proteins necessary for replication and virus production (33). Retrovirus vectors were originally produced as virus particles by using a replication-competent virus as a helper. Retrovirus vectors are now commonly produced as virus particles, with retrovirus helper (or packaging) cells. Helper cells contain the coding sequences for the viral proteins necessary for virus production but do not produce virus because of a partial or complete removal of the viral *cis*-acting sequences. The introduction of a retroviral vector into helper cells results in the production of vector virus that is free of helper virus (33).

One of the known *cis*-acting sequences necessary for virus production is the encapsidation (packaging) signal (E or Ψ) (41). The encapsidation signal of retroviruses is located primarily in the 5′ untranslated region of the genome and is necessary for the packaging of two identical copies of retroviral RNA into virus particles. The encapsidation signal for simpler retroviruses has been best characterized. Spleen necrosis virus (SNV) and murine leukemia virus (MLV) have a primary encapsidation signal that is located between the major splice donor site and the *gag* start codon (2, 4, 16, 31, 32, 49). However, an extended encapsidation signal, which increases viral RNA packaging and virus titer 10- to 200-fold, Ψ+, extends into the *gag* open reading frame for MLV (7, 37). The encapsidation signal for SNV and MLV is present only on the unspliced genomic RNA. The SNV E has been shown to form a double-hairpin structure (51). Rous sarcoma virus (RSV) has the major splice donor site just downstream of the *gag* start codon, and the primary encapsidation signal is located 5′ to the viral coding sequence (5, 6, 18, 25, 27, 50). Thus, the RSV encapsidation signal is located on both the unspliced and the spliced viral RNAs; however, the spliced *env* mRNA is only poorly encapsidated. The RSV encapsidation signal possibly extends into the *gag* region, including a region near the 3′ end of the genomic RNA (40, 45).

The encapsidation signals for the more complex retroviruses are not as well characterized as those for simpler retroviruses. The encapsidation signals for human immunodeficiency virus type 1 (HIV-1) and simian immunodeficiency virus appear to include the viral sequences upstream of the major splice donor site and the leader region between the major splice donor site and the *gag* start codon and may also extend into the 5′ end of the U5 region of the long terminal repeat (LTR) and the 3′ end of the *gag* coding sequence (3, 11, 20, 21, 29, 30, 38, 42). The efficiency of gene transfer has been found to increase by as much as 30-fold in HIV-1 vectors when over 600 nucleotides of the 5′ end of the *gag* gene are included (10, 38).

The encapsidation signal of human T-cell leukemia virus types I and II (HTLV-I and -II) and that of bovine leukemia virus (BLV) are poorly characterized. The exact location of the primary encapsidation signal for these more complex retroviruses has not been determined but may be either between the major splice donor site (in the r region of the viral RNA) and the *gag* start codon or between the primer binding site (located just downstream of the 5′ LTR) and the *gag* start codon. Sequences involved in dimerization of the viral genome (the dimer linkage sequence [DLS]) have been identified in vitro to be near the 5′ end of the viral RNA for BLV (23, 24). This region has been found to contain sequences or structures im-

* Corresponding author. Mailing address: McArdle Laboratory for Cancer Research, University of Wisconsin Medical School, 1400 University Ave., Madison, WI 53706. Phone: (608) 262-2024. Fax: (608) 262-2824. Electronic mail address: mansky@oncology.wisc.edu.

† This paper is dedicated to the memory of Howard M. Temin.

‡ Deceased.

portant for in vitro binding of the RNA to viral matrix-associated proteins, nucleocapsid protein, or the nucleocapsid domain of the Gag polyprotein precursor. With the exception of RSV, retroviral DLSs have been mapped in vivo to a region overlapping the E or Ψ (8, 12, 23, 35, 39, 46); this mapping has yet to be confirmed with viruses in the HTLV/BLV genus.

We have characterized sequences by deletion analysis that are necessary for efficient encapsidation of BLV RNA. The efficiency of RNA encapsidation revealed two important regions. The first region is a 132-nucleotide-base sequence within the *gag* gene that facilitates efficient RNA encapsidation in the presence of the second region. The second region includes sequences downstream of the primer binding site and near the *gag* gene start codon and is essential for RNA encapsidation. Our data support the conclusion that the encapsidation signal necessary for efficient RNA packaging and virus production is discontinuous.

MATERIALS AND METHODS

Nomenclature. Plasmid constructs are indicated by the letter p (e.g., pBLV-SVNEO) to distinguish them from virus (e.g., BLV-SVNEO). Most mutants of BLV-SVNEO are denoted with the symbol Δ followed by the nucleotide sequence coordinates of the first nucleotide of the restriction enzyme sites used to create deletions. The exception is the mutant Δ 1147, which was made as described below. The nucleotide sequence coordinates used are relative to the 5′ end of the proviral DNA for the complete BLV genome (43).

Construction of BLV vectors. All BLV vectors were constructed from pBLV-SVNEO (13). This plasmid was constructed from pBLV913, which contains a complete proviral copy of BLV derived from a fetal lamb kidney cell line producing wild-type BLV (FLK-BLV). pBLV-SVNEO contains a deletion of the *tax* and *rex* sequences and an insertion of the neomycin phosphotransferase gene (*neo*) driven by the simian virus 40 (SV40) early promoter (Fig. 1). This vector is not replication competent and requires that the BLV *tax* and *rex* genes be supplied in *trans*. BLV vectors (Fig. 1) were constructed with deletions in the *gag*, *pol*, and/or *env* coding sequences by digesting pBLV-SVNEO with various restriction endonucleases. For example, Δ 857-1147 was made by digestion of pBLV-SVNEO with *Msc*I and *Sal*I, Δ 698-1147 was made by digestion of pBLV-SVNEO with *Bss*HII and *Sal*I, and Δ 1015-2806 was made by digestion with *Eco*RV and *Sal*I. Two exceptions are vectors Δ 551-698 and Δ 698-1015, which also contain the deletion in mutant Δ 1147-6819. Digested DNAs with incompatible ends were made blunt ended with the Klenow fragment of DNA polymerase (Boehringer Mannheim, Indianapolis, Ind.) and then were ligated with T4 DNA ligase (Boehringer Mannheim). Digested DNAs with compatible ends were religated with T4 DNA ligase. All ligated DNAs were electroporated into the DH5α strain of *Escherichia coli* and plated on appropriate selective media. Deletion junctions from ligations of digested DNAs with incompatible ends were confirmed by DNA sequence analysis.

Cell lines, transfections, and cocultivations. Madin-Darby bovine kidney (MDBK) cells were used to test virus production by use of helper plasmids. FLK-BLV cells (graciously provided by Martin Van der Maaten, National Animal Disease Center, Ames, Iowa) were used to test virus production by use of BLV helper virus. FLK-BLV cells produce all the BLV proteins necessary for virus production and have been used previously for vector virus production (48). All cells were grown in Temin modified Eagle's medium (47) supplemented with 10% fetal bovine serum (Sigma Chemical Co., St. Louis, Mo.). MDBK and FLK-BLV cells were transfected by the dimethyl sulfoxide-Polybrene procedure as previously described (26).

FLK-BLV cells were transfected with each of the vectors tested. Two days posttransfection, cells were placed under G418 selection. Approximately 100 G418-resistant colonies were pooled and used for cocultivation with FLK target cells. FLK cells free of BLV (kindly supplied by Judy Mikovits, National Cancer Institute, Frederick, Md.) were used as target cells. Infection of target cells was done by cocultivation of virus-producing cells with target cells as described by Mansky and Temin (34). Briefly, virus-producing cells (typically 2.5×10^5 cells in a 60-mm-diameter petri dish) were treated with mitomycin (10 μg/ml), an inhibitor of host cell DNA synthesis, for 2 h at 37°C. The cells were then washed three times with fresh medium, and 2.5×10^5 FLK target cells were added. Two days after cocultivation, selective medium containing G418 was added. Control experiments were done with each cocultivation experiment to ensure that mitomycin-treated, virus-producing cells did not proliferate and no longer adhered to the surfaces of culture dishes.

Production of vector virus by *trans* complementation with helper plasmids. A BLV *gag-pol* expression plasmid, pAK4, was constructed to complement in *trans* BLV vectors with mutations in *gag-pol* (Fig. 2). This was done in several steps. First, the *gag-pol* region (nucleotides 628 to 4880) of pBLV-SVNEO was amplified by PCR, with primers containing restriction enzyme sites for *Sph*I. Second, the PCR product was digested with *Sph*I and purified in a Chroma Spin-100 column (Clontech Laboratories, Palo Alto, Calif.). The digested PCR DNA was cloned into the *Sph*I site of pUC19. Third, the *Sph*I fragment was digested from this plasmid and cloned into the *Sph*I site of pJDCMV19SV (15), a plasmid that contains the cytomegalovirus immediate-early promoter and the simian virus 40 polyadenylation signal sequence to create pAK4. This plasmid, along with a BLV *tax/rex* expression plasmid, pBLPX-RSPA (kindly provided by David Derse, National Cancer Institute, Frederick, Md.), and an amphotropic MLV *env* expression plasmid, pSV-A-MLV-env (kindly supplied by Dan Littman, University of California, San Francisco) (28), was transfected into MDBK cells with pTG76, a plasmid that expresses the hygromycin B phosphotransferase gene (*hyg*) under the control of the SV40 early promoter (19). After transfection, cells were placed under hygromycin selection (330 μg/ml). Individual hygromycin-resistant cell clones were isolated and were screened by PCR for the presence of the introduced expression plasmids with the appropriate primer sets for each plasmid.

Virus production from individual MDBK cell clones was tested for transfer of BLV vector virus to FLK target cells. First, cell clones were transfected with pBLV-SVNEO or with one of the deletion mutants and were selected 2 days later in media containing G418. Second, vector virus was then transferred to fresh MDBK cells containing helper plasmids by cocultivation. After cocultivation, cells were placed under G418 selection in medium containing α-BLV antisera and a monoclonal antibody directed against the amphotropic MLV envelope protein (kindly supplied by Leonard Evans, Rocky Mountain Laboratory, National Institute of Allergy and Infectious Diseases, Hamilton, Mont.) to prevent virus spread. Third, transfer of vector virus to FLK target cells was done by cocultivation. Vector virus from infected helper cells rather than from transfected helper cells was used for virus transfer because of mutations arising from the transfection process (14). Control experiments were done with each cocul-

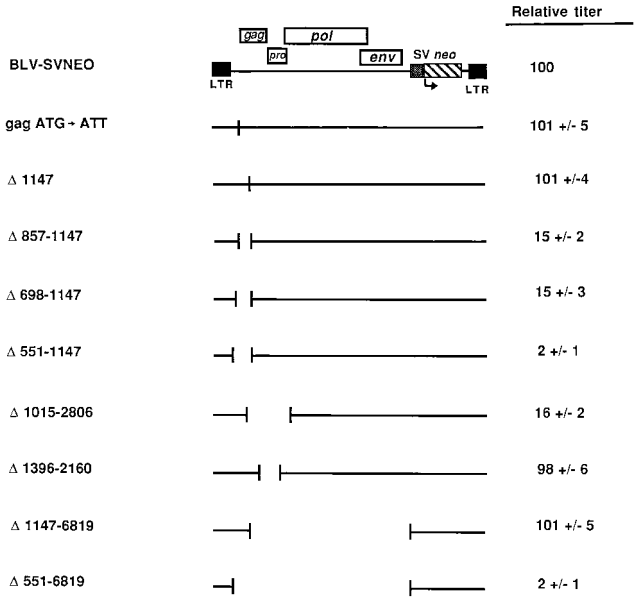

FIG. 1. Deletion analysis of a BLV vector for testing the efficiency of virus replication with a BLV helper virus. Vector virus produced from stably transfected FLK-BLV cells was used to infect FLK target cells by cocultivation as described in Materials and Methods. The BLV vector BLV-SVNEO is shown in proviral DNA form. Mutant vectors are denoted with the symbol Δ followed by the nucleotide sequence coordinates of the first nucleotide of the restriction enzyme sites used to create the deletion. The nucleotide sequence coordinates used are relative to the 5′ end of the proviral DNA for the complete BLV genome (43). Solid black boxes represent BLV LTRs. Solid black lines indicate viral sequence. Rectangular boxes above the solid black lines indicate viral coding sequences, with the vertical locations of the boxes corresponding to the translational reading frame. Retroviral genes are indicated as *gag*, *pro*, *pol*, and *env*. The SV40 promoter is represented as a dark gray box; the *neo* gene is represented as a hatched rectangular box. Mutants of BLV-SVNEO are represented as solid black lines, with black vertical lines indicating restriction enzyme sites that were used to make the deletions; deleted sequences in each mutant are represented as the space between the black vertical lines. The titer data presented are from three independent experiments, with the relative titers (normalized to BLV-SVNEO) presented as the average ± standard deviation. The average absolute titer of BLV-SVNEO from these three experiments was 4×10^2 CFU per 5×10^4 FLK target cells.

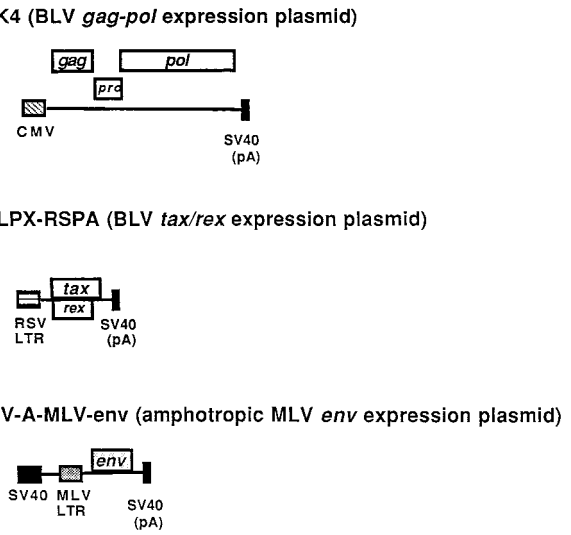

FIG. 2. Expression plasmids used for vector virus production. The viral coding sequences and regulatory elements from each plasmid are shown. Solid black lines indicate viral sequence. Rectangular boxes above or below the solid black lines indicate the viral coding sequences, with the boxes indicating open reading frames for the BLV *gag*, *pro*, *pol*, *tax*, and *rex* genes and the amphotropic MLV (A-MLV) *env* gene (shown as a light-gray box). The solid black box represents the SV40 promoter, the cross-hatched box represents the cytomegalovirus (CMV) promoter, and the medium-gray box represents the A-MLV promoter. The box with horizontal lines represents the RSV LTR. The thin black box indicates the SV40 late gene polyadenylation signal [SV40 (pA)].

tivation experiment to ensure that mitomycin-treated, virus-producing cells did not proliferate and no longer adhered to the surfaces of culture dishes.

Determination of cytoplasmic and virion RNA levels of mutant vectors. Levels of vector viral RNA in cells and in virions were determined by RNA slot blot analysis. Cytoplasmic RNA was harvested from pools of G418-resistant clones that had been infected by cocultivation with deletion mutants of BLV-SVNEO. Cytoplasmic RNA was purified with guanidine hydrochloride from a commercially available RNA isolation kit (RNAgents kit; Promega Corp., Madison, Wis.). Virion RNA was purified from virions pelleted from cleared supernatant medium by ultracentrifugation in a 70.1Ti rotor at 50,000 rpm for 1 h. Virion pellets were resuspended in buffer containing 150 mM NaCl, 10 mM Tris (pH 7.4), 1 mM EDTA, 0.5% sodium dodecyl sulfate, and 100 μg of tRNA per ml. Proteinase K was added to a final concentration of 50 μg/ml, and samples were incubated at 37°C for 10 min and then immediately frozen. The virion RNA was then purified by phenol-chloroform extraction and ethanol precipitation (44).

Cytoplasmic and virion RNAs were denatured at 65°C for 15 min. Samples were twofold serially diluted in 20× SSC (1× SSC is 0.15 M NaCl plus 0.015 M sodium citrate) and were blotted onto nitrocellulose paper (Schleicher & Schuell, Keene, N.H.) with a slot blot vacuum manifold (Millipore, Bedford, Mass.). The blots were then baked under vacuum at 80°C for 2 h.

A DNA probe representing the U5 region of the 5′ end of the viral RNA, which is downstream from the splice donor site for the *env* mRNA, was used for hybridizations. The DNA probe was PCR amplified from pBLV-SVNEO and resolved in a 1% agarose gel. This probe DNA was then gel purified with an NA45 membrane (Schleicher & Schuell) and was labeled by random priming (Random Primed DNA Labeling Kit; Boehringer Mannheim). Hybridization was done under standard conditions (44). Hybridization was visualized, and relative intensities were quantified with a phosphoimager (Molecular Dynamics, Sunnyvale, Calif.).

Computer analysis of potential RNA secondary structures. The GCG programs (version 8; Genetics Computer Group, Madison, Wis.) FoldRNA (53) and MFold (22, 52) were used for the analysis of minimal free energy and suboptimal RNA secondary structures of the RNA sequence in the *gag* gene region between nucleotides 700 and 1150 of the proviral DNA. The RNA structures predicted by FoldRNA and MFold were plotted with the GCG programs Squiggles and Plotfold, respectively. The calculation of minimal free energy was performed with the Turner energies (17). The Star program (1) was used to analyze potential pseudoknot structures.

RESULTS

Grouping of deletion mutants on the basis of the efficiency of virus replication. We made various deletions in BLV-SVNEO in order to determine the effects of these deletions on virus replication and to define vectors that contained a minimal amount of viral coding sequence. The ability of these vectors to replicate was initially tested with a BLV helper virus as described in Materials and Methods. FLK-BLV cells were stably transfected with each of the deletion mutants. About equal numbers of G418-resistant colonies were observed for each mutant vector per microgram of transfected plasmid DNA (data not shown). Approximately 100 G418-resistant colonies were pooled for each mutant and used for cocultivation with FLK target cells.

Figure 1 shows the results of vector virus production from FLK-BLV cells. The titers of vector virus mutants allow the mutants to be grouped into three classes. The first group of mutants had titers that were lower than the parental vector by about a factor of seven. A second group of mutants had titers that were lower by about a factor of 50 than that of the parental vector. Finally, a third group had vector virus titers that were similar to those of the parental vector.

Three deletion mutants had mutations in the 5′ end of the *gag* gene that led to a reduction in the level of vector virus transfer compared with that in the parental vector. Mutants Δ 857-1147, Δ 698-1147, and Δ 1015-2806 had a reduction in vector virus titer by about a factor of seven. The titer of these vectors suggests that a portion of the encapsidation signal was removed for efficient virus production but that the primary encapsidation signal was not removed. These mutants suggest that a 132-nucleotide-base region between nucleotides 1015 and 1147 of the proviral DNA might contain the deleted portion of the encapsidation signal.

Two deletion mutants had drastic reductions in the titer relative to the parental vector. Vector virus production of mutant Δ 551-1147, which contains a deletion of the 5′ untranslated region directly after the BLV primer binding site and the 5′ end of the *gag* gene, was reduced by about a factor of 50. The mutant Δ 551-6819 has a deletion of the *gag*, *pol*, and *env* genes along with deletion of the 5′ untranslated leader region immediately after the BLV primer binding site. The titer of Δ 551-6819 was also reduced by about a factor of 50. The position of the mutations in these vectors suggests that the encapsidation signal was deleted.

Several deletion mutants had virus titers comparable to those of the parental vector. The mutant pgagATG→ATT contains a single base substitution changing the start codon of the *gag* gene from ATG to ATT. The mutant pΔ 1147 has an additional four nucleotides in the *gag* gene and a subsequent +1 frameshift in the translational reading frame. This leads to an opal stop codon 16 amino acids downstream of the mutation. These mutations had no effect on virus production compared with production of BLV-SVNEO, indicating that Gag could be supplied in *trans*. Truncation of Gag did not affect virus production of Δ 1147, suggesting that dominant interference with virus replication by the truncated Gag protein did not occur. Virus production of mutant Δ 1396-2160, containing a deletion of the 3′ end of the *gag* gene, was equal to that of BLV-SVNEO. Deletion mutations of sequences in the *pol* gene, mutant Δ 3282-6819, and larger deletions spanning the *gag* and *pol* coding sequences (mutants Δ 3205-6819 and Δ 1875-6819) had no effect on the efficiency of virus production compared with that of BLV-SVNEO (data not shown). A mutant containing a deletion of a portion of the *gag* and all of the *pol* and *env* coding sequences, Δ 1147-6819, also had no effect on the efficiency of virus production (Fig. 1).

Replication efficiency of 5′-end *gag* mutants in a single round of retrovirus replication. The mutants produced from FLK-BLV cells may have undergone multiple rounds of rep-

TABLE 1. Relative titers of 5′-end *gag* mutants produced with helper plasmids[a]

Deletion mutant	Relative titer[b]
Δ 1015-2806	15 ± 4
Δ 698-1147	16 ± 3
Δ 857-1147	16 ± 4
BLV-SVNEO[c]	100

[a] Data are from three independent experiments. Two experiments were done with helper cell clone 1A; one experiment was done with helper cell clone 2A.
[b] Relative titers (normalized to values for BLV-SVNEO) are presented as the average ± standard deviation.
[c] The average absolute titer of BLV-SVNEO from these three experiments was 7×10^2 CFU per 5×10^4 FLK target cells.

lication. Mutants were produced with helper cells to test the effect of the mutations on the replication efficiency of vector virus in a single round of replication in the absence of competing helper viral RNA. A BLV helper cell line was made by introducing helper plasmids (Fig. 2) into the MDBK cell line by transfection. A BLV *gag-pol* expression plasmid (pAK4), a BLV *tax/rex* expression plasmid (pBLPX-RSPA), and an amphotropic MLV *env* expression plasmid (pSV-A-MLV-env) were transfected into cells with pTG 76, a plasmid that contains *hyg* under the control of the SV40 promoter. Cells were placed under selection for hygromycin resistance. Single, well-isolated colonies were then picked and expanded. The resulting cell clones were screened by PCR for the presence of pAK4, pBLPX-RSPA, and pSV-A-MLV-env.

To determine whether these cells could act as helper cells for BLV-based vectors, two different cell clones were transfected with pBLV-SVNEO or with the deletion mutant pΔ 857-1147, pΔ 698-1147, or pΔ 1015-2806. About equal numbers of drug-resistant colonies were observed for each mutant vector per microgram of transfected plasmid DNA (data not shown). Vector virus produced from these cells was transferred to fresh helper cells by cocultivation, rather than infection by transferring supernatants from virus-producing cells, because of the low titer of BLV vectors (~5 to 40 CFU/ml) (34). Mitomycin was used to block cell division and replication of the virus-producing cells. In each cocultivation experiment, control experiments were done to ensure that the mitomycin-treated, virus-producing cells did not proliferate and no longer adhered to the surfaces of culture dishes. Pools of these vector virus-producing cells (2.5×10^5 cells, typically from over 100 drug-resistant colonies) were then used in cocultivation with FLK target cells. BLV-SVNEO virus was produced at levels comparable to that produced from FLK-BLV cells (Table 1). Virus production of the deletion mutants was found to be about one-seventh of that of BLV-SVNEO, as was observed with the FLK-BLV cells.

Proper construction of these helper cells was confirmed by several different methods. First, G418-resistant FLK target cells were maintained through multiple passages, and supernatant from the growth medium was screened at each passage for detection of BLV reverse transcriptase activity (data not shown). We found after five passages of eight independent clones for each vector (produced from one of the helper cell clones) that no reverse transcriptase activity was detected, indicating that no replication-competent BLV was produced by the helper cells. Second, we used PCR to determine the integrity of the vector provirus of each deletion mutant and the parental BLV-SVNEO in target cells. We found, with various primer sets, that the integrity of the vector provirus was maintained, indicating that no genetic rearrangements of the vector virus had occurred (data not shown). Third, when target cells were infected with wild-type BLV and virus was harvested to infect fresh target cells, we found that G418 resistance was transferred to the infected cells, which provided further evidence that the vector proviral DNA was of the proper structure (data not shown).

Analysis of RNA packaging efficiency. To determine whether RNA packaging efficiency was reduced in the 5′-end *gag* mutant vectors, viral RNA levels of mutants Δ 857-1147, Δ 698-1147, and Δ 1015-2806 were compared with viral RNA levels of BLV-SVNEO by RNA slot blot analysis (Fig. 3). Cytoplasmic vector RNA levels in cells producing mutants of BLV-SVNEO, with a probe to the U5 region, were found to be comparable to the RNA levels observed in cells producing the parental BLV-SVNEO (Fig. 3A). Amounts of vector RNA from virions containing these three deletion mutants were reduced relative to those of BLV-SVNEO (Fig. 3B). Similar results were found

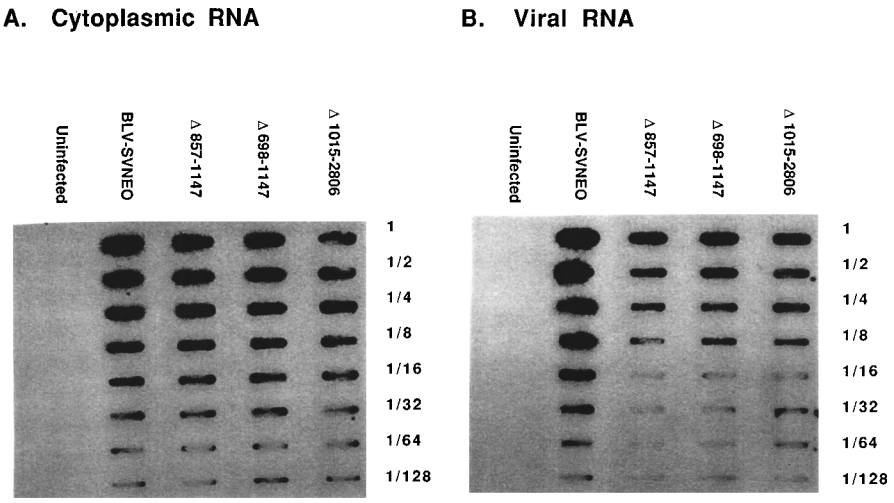

FIG. 3. Analysis of relative cytoplasmic and virion RNA levels. (A) Cytoplasmic RNA. RNA from five petri dishes (diameter, 100 mm) of infected or uninfected cells was twofold serially diluted and blotted onto nitrocellulose paper. The blot was probed with a randomly primed U5 probe. (B) Virion RNA. RNA from the equivalent of the supernatant medium from 20 petri dishes (diameter, 100 mm) (200 ml total) was twofold serially diluted and blotted. The probe used was a randomly primed U5 probe.

TABLE 2. Relative titers of deletion mutant vectors that locate the 3′ end of the primary encapsidation signal[a]

Deletion mutant	Relative titer[b]
Δ 551-698[c]	2 ± 2
Δ 698-1015	82 ± 5
Δ 1147-6819	101 ± 7
BLV-SVNEO[d]	100

[a] Data are from three independent experiments. Helper cell clone 1A was used in each experiment.
[b] See Table 1, footnote *b*.
[c] The deletion mutants Δ 551-698 and Δ 698-1015 also contain the mutation in deletion mutant Δ 1147-6819.
[d] See Table 1, footnote *c*.

with probes to the *pol* region and to the *neo* region (data not shown). This reduction in encapsidation efficiency is comparable to the reduction observed with virus production of these mutants. Therefore, less-efficient packaging of the mutant RNA is responsible for the observation of lower levels of virus production for these mutants. The RNA packaging efficiency of BLV-SVNEO from helper cells is about 10-fold higher than the packaging efficiency of this vector from FLK-BLV cells (data not shown), indicating that BLV-SVNEO RNA is able to compete well with wild-type BLV RNA for packaging into virus particles.

Locating the 3′ end of the primary encapsidation signal. To help locate the 3′ end of the primary encapsidation signal, we constructed two deletion mutants containing deletions in the region between nucleotides 551 and 1015, Δ 551-698 and Δ 698-1015. Each of these deletions was derived from the mutant Δ 1147-6819. Virus production of these mutants was tested by transfer from BLV helper cells to FLK target cells, as done with the other deletion mutants tested. Mutant Δ 1147-6819 was produced at levels comparable to that produced from FLK-BLV cells (Table 2). Virus production of mutant Δ 698-1015 was 80% of the virus production of Δ 1147-6819 and BLV-SVNEO. Mutant Δ 551-698 virus production was reduced by a factor of 50 relative to that of Δ 1147-6819 and BLV-SVNEO. Viral RNA levels of these mutants were determined by RNA slot blot analysis with a probe to the U5 region

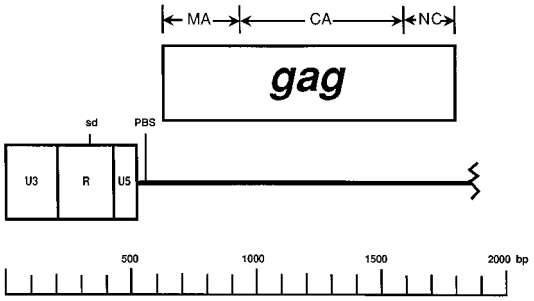

FIG. 5. The 5′ end of the BLV-SVNEO genome. BLV-SVNEO is shown in proviral DNA form. The rectangular box at the end of the solid black line represents the 5′ BLV LTR containing the U3 region, the R region, and the U5 region. The solid black line indicates the viral sequence. The locations of the major splice donor site (sd) and the primer binding site (PBS) are indicated. The rectangular box above the solid black lines indicates the BLV *gag* gene. The matrix (MA), capsid (CA), and nucleocapsid (NC) domains of *gag* are indicated above the rectangular box. The jagged line at the end of the viral coding sequence indicates the end of the viral sequence shown in this diagram.

(Fig. 4). Amounts of vector RNA from virions of mutant Δ 698-1015 were reduced by 20% relative to that of Δ 1147-6819 and BLV-SVNEO. Vector RNA from virions of mutant Δ 551-698 was reduced by more than a factor of 50 relative to that of Δ 1147-6819 and BLV-SVNEO (Fig. 4).

Analysis of potential RNA secondary structures. The BLV RNA in the region between nucleotides 700 and 1150 of the proviral DNA (Fig. 5) was analyzed for suboptimal and minimal free-energy structures. The predicted RNA secondary structure shown in Fig. 6 represents a minimum-energy optimal folding in this region from nucleotides 1042 to 1090. This structure lies within the 132-nucleotide-base region (nucleotides 1015 to 1147) that was mapped as being necessary for efficient virus production and RNA packaging. The same structure was also predicted with suboptimal folding. No pseudoknot foldings were predicted for the unusually large loop sequence with adjacent sequences by use of the STAR program (1).

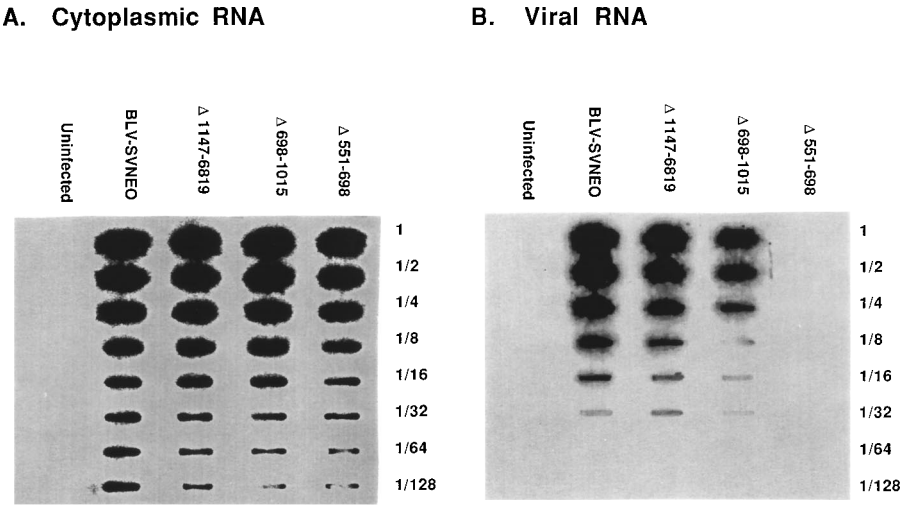

FIG. 4. Location of the 3′ end of the primary encapsidation signal. (A) Cytoplasmic RNA. RNA from five petri dishes (diameter, 100 mm) of infected or uninfected cells was twofold serially diluted and blotted onto nitrocellulose paper. The blot was probed with a randomly primed U5 probe. (B) Virion RNA. RNA from the equivalent of the supernatant medium from 20 petri dishes (diameter, 100 mm) (200 ml total) was twofold serially diluted and blotted. The probe used was a randomly primed U5 probe.

DISCUSSION

A series of deletion mutants, based on the BLV vector BLV-SVNEO, was constructed to define vectors that contained a minimal amount of viral coding sequence. We initially tested the replication efficiency of these mutants by transfection into FLK-BLV cells. We found that deletions in the 5′ end of the *gag* gene led to a reduction in replication efficiency by a factor of about seven. Deletions including the 5′ untranslated leader region led to a reduction in replication by a factor of about 50. Deletions of the 3′ end of the *gag* gene, the *pol* gene, and the *env* gene had no effect on replication of the vector virus. We confirmed and extended these observations by determining the replication efficiency of mutants from BLV helper cells and by measuring the efficiency of RNA encapsidation into virus particles.

Mutants that contained deletions in the 5′ end of the *gag* gene of BLV-SVNEO (i.e., Δ 857-1147, Δ 698-1147, and Δ 1015-2806) lowered the level of virus replication from FLK-BLV cells by a factor of seven compared with that of BLV-SVNEO. Similar results were obtained when vector virus of the mutants was produced from BLV helper cells. These results indicate that the nucleotide sequence that increases the efficiency of virus replication extends into a 132-nucleotide-base region between nucleotides 1015 and 1147 in the proviral DNA of the *gag* gene in BLV-SVNEO (Fig. 5). This region lies within the capsid-encoding domain of the *gag* gene. Further analysis indicated that these mutants exhibited a decreased encapsidation efficiency.

Our results indicate, as has also been suggested with MLV and HIV-1 vectors, that BLV vectors containing the 5′ end of the *gag* gene have higher titers. This indicates that the encapsidation signal extends into the *gag* gene. The increase in virus replication observed is significant because of the generally low titers of the BLV vectors. The 3′ end of the primary BLV encapsidation signal was located by constructing two mutants, Δ 551-698 and Δ 698-1015. Deletion of the region between nucleotides 551 and 698 reduced the level of RNA encapsidation and virus production by about a factor of 50. Deletion of the region between nucleotides 698 and 1015 reduced RNA packaging and virus production by 20% compared with that of the parental vector. This indicates that the 3′ end of the primary BLV encapsidation signal is positioned before nucleotide 698 near the *gag* start codon (*gag* begins at nucleotide 628). The encapsidation signal necessary for efficient viral RNA encapsidation appears discontinuous, as deletion of the region between nucleotides 698 and 1015 reduced the level of RNA encapsidation by only 20% compared with that of the parental vector. This observed reduction may indicate that sequences necessary for efficient RNA encapsidation may be located within the region between nucleotides 698 and 1015. However, this reduction is minimal relative to the factor of 7 and factor of 50 reductions in RNA encapsidation observed with other mutants. Therefore, these results are consistent with the BLV encapsidation signal having a primary signal located mainly in the 5′ untranslated leader region and an extended region in the *gag* gene.

The 147-nucleotide-base region between nucleotides 551 and 698 may not contain the entire primary encapsidation signal, as chimeric vectors between BLV and SNV indicate that the BLV U5 region increases virus production and RNA encapsidation by a factor of 4 (9). The HIV-1 and simian immunodeficiency virus encapsidation signals appear to extend into the 5′ end of the U5 region of the LTR (3, 11, 20, 21, 29, 30, 38, 42). Adding the BLV sequences necessary for efficient RNA encapsidation to nonretroviral RNAs would help identify the BLV encapsidation signal that is sufficient for encapsidation, as has been done with simpler retroviruses (2).

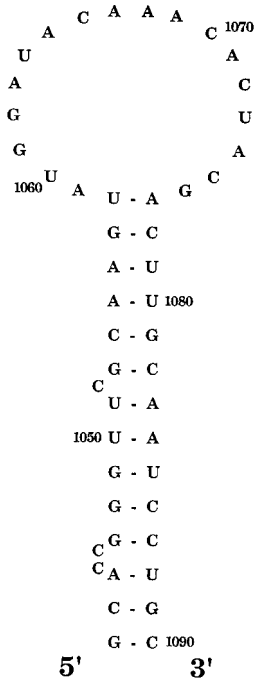

FIG. 6. RNA secondary structure predicted in the extended encapsidation signal by computer-assisted analysis of suboptimal and minimal free-energy folding. The region shown is located within a 132-nucleotide-base region between nucleotides 1015 and 1147 in the *gag* gene of the genomic viral RNA. The nucleotide base numbering is based on the complete BLV proviral DNA genome (43).

Our results suggest that the primary encapsidation signal overlaps with two structures in the viral RNA that are important for in vitro dimer formation (nucleotides 445 to 574) and matrix-associated protein binding (nucleotides 628 to 682) (23, 24). DLSs for other retroviruses have been mapped in vivo to a region overlapping the E or Ψ (8, 12, 24, 35, 39, 46).

Milan and Nicolas (36) reported that inclusion of a large portion of the BLV *gag* gene in BLV-based vectors did not significantly increase the titer. Determination of virion RNA levels for these vectors was not carried out. Also, no vectors that had a lower titer were described. Therefore, it is not possible to directly compare these findings with our results. It is also possible that a step other than encapsidation is rate limiting in their system.

RNA secondary structures have been implicated as being important for the function of retroviral encapsidation signals (51). We reasoned that such structures may exist in the regions we have mapped and may be important for efficient RNA packaging and virus production. Two RNA secondary structures predicted for dimer formation and binding of the BLV matrix protein have been proposed (24) and may overlap with the primary BLV encapsidation signal. We analyzed the region in the *gag* gene between nucleotides 700 and 1150 for suboptimal and minimal free-energy structures. The predicted RNA secondary structure (Fig. 6) represents the minimal free-energy folding of a region from nucleotides 1042 to 1090. The nucleotides that form this structure are within the 132-nucleotide-base region (i.e., the region from nucleotides 1015 to 1147 of the proviral DNA) that was mapped as being secondary for efficient virus production and RNA packaging. The same structure was also predicted with the suboptimal folding.

The structure that we have identified was predicted with two other BLV isolates (data not shown). Each isolate contained two nucleotide changes that maintained the stem structure, indicating that the stem structure may be conserved. To determine if the sequences in the large loop sequence base paired with adjacent sequences, we tested this region for pseudoknot foldings with the STAR program. No likely pseudoknot foldings were predicted. However, we believe that pseudoknot structures that were not predicted by the program used could exist. It is unknown whether the predicted structures within the regions of the primary encapsidation signal (24) and the extended encapsidation signal (Fig. 6) are important for efficient RNA packaging and virus production.

ACKNOWLEDGMENTS

We thank Xiao-Juan Bi, Timothy Jacoby, and Brad Seufzer for technical assistance; Kathy Boris-Lawrie, Dawn Burns, Gary Pulsinelli, Bill Sugden, and Shiaolan Yang for helpful discussions and comments on the manuscript; and Nito Panganiban for critical reading of the manuscript.

This work was supported by grants CA22443 and CA07175 from the Public Health Service. L.M.M. was supported by NRSA Viral Oncology training grant CA09075-17 and by an NIH postdoctoral fellowship. H.M.T. was an American Cancer Society Research Professor.

REFERENCES

1. **Abrahams, J. P., M. van den Berg, E. van Batenburg, and C. Pleij.** 1990. Prediction of RNA secondary structure, including pseudoknotting, by computer simulation. Nucleic Acids Res. **18:**3035–3044.
2. **Adam, M. A., and A. D. Miller.** 1988. Identification of a signal in a murine retrovirus that is sufficient for packaging of nonretroviral RNA into virions. J. Virol. **62:**3802–3806.
3. **Aldovini, A., and R. A. Young.** 1990. Mutations of RNA and protein sequences involved in human immunodeficiency virus type 1 packaging result in production of noninfectious virus. J. Virol. **64:**1920–1926.
4. **Armentano, D., S.-F. Yu, P. W. Kantoff, T. von Ruden, W. F. Anderson, and E. Gilboa.** 1987. Effect of internal viral sequences on the utility of retroviral vectors. J. Virol. **61:**1647–1650.
5. **Aronoff, R., A. M. Hajjar, and M. L. Linial.** 1993. Avian retroviral RNA encapsidation: reexamination of functional 5′ RNA sequences and the role of nucleocapsid Cys-His motifs. J. Virol. **67:**178–188.
6. **Aronoff, R., and M. Linial.** 1991. Specificity of retroviral RNA packaging. J. Virol. **65:**71–80.
7. **Bender, M. A., T. D. Palmer, R. E. Gelinas, and A. D. Miller.** 1987. Evidence that the packaging signal of Moloney murine leukemia virus extends into the *gag* gene. J. Virol. **61:**1639–1646.
8. **Bieth, E., C. Gabus, and J.-L. Darlix.** 1990. A study of the dimer formation of Rous sarcoma virus RNA and of its effect on viral protein synthesis *in vitro*. Nucleic Acids Res. **18:**119–127.
9. **Boris-Lawrie, K., and H. M. Temin.** 1995. Genetically simpler bovine leukemia virus derivatives can replicate independently of Tax and Rex. J. Virol. **69:**1920–1924.
10. **Buchschacher, G. L., Jr., and A. T. Panganiban.** 1992. Human immunodeficiency virus vectors for inducible expression of foreign genes. J. Virol. **66:**2731–2739.
11. **Clavel, F., and J. M. Orenstein.** 1990. A mutant of human immunodeficiency virus with reduced RNA packaging and abnormal particle morphology. J. Virol. **64:**5230–5234.
12. **Darlix, J.-L., C. Gabus, M.-T. Nugeyre, F. Clavel, and F. Barré-Sinoussi.** 1990. *cis* elements and *trans*-acting factors involved in the RNA dimerization of the human immunodeficiency virus HIV-1. J. Mol. Biol. **216:**689–699.
13. **Derse, D., and L. Martarano.** 1990. Construction of a recombinant bovine leukemia virus vector for analysis of virus infectivity. J. Virol. **64:**401–405.
14. **Dougherty, J. P., and H. M. Temin.** 1986. High mutation rate of a spleen necrosis virus-based retrovirus vector. Mol. Cell. Biol. **68:**4387–4395.
15. **Dougherty, J. P., R. Wisniewski, S. Yang, B. W. Rhode, and H. M. Temin.** 1989. New retrovirus helper cells with almost no nucleotide sequence homology to retrovirus vectors. J. Virol. **63:**3209–3212.
16. **Embretson, J. E., and H. M. Temin.** 1987. Lack of competition results in efficient packaging of heterologous murine retroviral RNAs and reticuloendotheliosis virus encapsidation-minus RNAs by the reticuloendotheliosis virus helper cell line. J. Virol. **61:**2675–2683.
17. **Freier, S. M., R. Kierzek, J. A. Jaeger, N. Sugimito, M. H. Caruthers, T. Neilson, and D. H. Turner.** 1986. Improved free-energy parameters for predictions of RNA duplex stability. Proc. Natl. Acad. Sci. USA **83:**9373–9377.
18. **Gallis, B., M. Linial, and R. Eisenman.** 1979. An avian oncovirus mutant deficient in genomic RNA: characterization of the packaged RNA as cellular messenger RNA. Virology **94:**146–161.
19. **Giordano, T. J., and W. T. McAllister.** 1990. Optimization of the hygromycin B resistance-conferring gene as a dominant selectable marker in mammalian cells. Gene **88:**285–288.
20. **Harrison, G. P., and A. M. L. Lever.** 1992. The human immunodeficiency virus type 1 packaging signal and major splice donor region have a conserved stable secondary structure. J. Virol. **66:**4144–4153.
21. **Hayashi, T., T. Shisuo, Y. Iwakura, and H. Shibuta.** 1992. RNA packaging signal of human immunodeficiency virus type 1. Virology **188:**590–599.
22. **Jaeger, J. A., D. H. Turner, and M. Zuker.** 1989. Improved predictions of secondary structures for RNA. Proc. Natl. Acad. Sci. USA **86:**7706–7710.
23. **Katoh, I., H. Kyushiki, Y. Sakamoto, Y. Ikawa, and Y. Yoshinaka.** 1991. Bovine leukemia virus matrix-associated protein MA(p15): further processing and formation of a specific complex with the dimer of the 5′-terminal genomic RNA fragment. J. Virol. **65:**6845–6855.
24. **Katoh, I., T. Yasunaga, and Y. Yoshinaka.** 1993. Bovine leukemia virus RNA sequences involved in dimerization and specific *gag* protein binding: close relation to the packaging sites of avian, murine, and human retroviruses. J. Virol. **67:**1830–1839.
25. **Katz, R. A., R. W. Terry, and A. M. Skalka.** 1986. A conserved *cis*-acting sequence in the 5′ leader of avian sarcoma virus RNA is required for packaging. J. Virol. **59:**163–167.
26. **Kawai, S., and M. Nishizawa.** 1984. New procedure for DNA transfection with polycation and dimethyl sulfoxide. Mol. Cell. Biol. **4:**1172–1174.
27. **Koyama, T., F. Harada, and S. Kawai.** 1984. Characterization of Rous sarcoma virus mutant defective in packaging its own genomic RNA: biochemical properties of mutant TK15 and mutant-induced transformants. J. Virol. **51:**154–162.
28. **Landau, N. R., and D. R. Littman.** 1992. Packaging system for rapid production of murine leukemia virus vectors with variable tropism. J. Virol. **66:**5110–5113.
29. **Lever, A., H. Gottlinger, W. Haseltine, and J. Sodroski.** 1989. Identification of a sequence required for efficient packaging of human immunodeficiency virus type 1 RNA into virions. J. Virol. **63:**4085–4087.
30. **Luban, J., and S. P. Goff.** 1994. Mutational analysis of *cis*-acting packaging signals in human immunodeficiency virus type 1 RNA. J. Virol. **68:**3784–3793.
31. **Mann, R., and D. Baltimore.** 1985. Varying the position of a retrovirus packaging sequence results in the encapsidation of both unspliced and spliced RNAs. J. Virol. **54:**401–407.
32. **Mann, R., R. C. Mulligan, and D. Baltimore.** 1983. Construction of a retrovirus packaging mutant and its use to produce helper-free defective retrovirus. Cell **33:**153–159.
33. **Mansky, L. M.** 1994. Retroviral-vector-mediated gene transfer, p. 27B:5.1–27B:5.10. *In* J. B. Griffiths, A. Doyle, and D. G. Newell (ed.), Cell and tissue culture: laboratory procedures. John Wiley & Sons, Inc., New York.
34. **Mansky, L. M., and H. M. Temin.** 1994. Lower mutation rate of bovine leukemia virus relative to that of spleen necrosis virus. J. Virol. **68:**494–499.
35. **Marquet, R., F. Baudin, C. Gabus, J.-L. Darlix, M. Mougel, C. Ehresmann, and B. Ehresmann.** 1991. Dimerization of human immunodeficiency virus (type 1) RNA: stimulation by cations and possible mechanism. Nucleic Acids Res. **19:**2349–2357.
36. **Milan, D., and J.-F. Nicolas.** 1991. Activator-dependent and activator-independent defective recombinant retroviruses from bovine leukemia virus. J. Virol. **65:**1938–1945.
37. **Osborne, W. R. A., and A. D. Miller.** 1988. Design of vectors for efficient expression of human purine nucleoside phosphorylase in skin fibroblasts from enzyme-deficient humans. Proc. Natl. Acad. Sci. USA **85:**6851–6855.
38. **Parolin, C., T. Dorfman, G. Palu, H. Gottlinger, and J. Sodroski.** 1994. Analysis in human immunodeficiency virus type 1 vectors of *cis*-acting sequences that affect gene transfer into human lymphocytes. J. Virol. **68:**3888–3895.
39. **Prats, A.-C., C. Roy, P. Wang, M. Erard, V. Housset, C. Gabus, C. Paoletti, and J.-L. Darlix.** 1990. *cis* elements and *trans*-acting factors involved in dimer formation of murine leukemia virus RNA. J. Virol. **64:**774–783.
40. **Pugatsch, T., and D. W. Stacey.** 1983. Identification of a sequence likely to be required for avian retroviral packaging. Virology **128:**505–511.
41. **Rein, A.** 1994. Retroviral RNA packaging: a review. Arch. Virol. **9**(Suppl.)**:** 513–522.
42. **Rizvi, T. A., and A. T. Panganiban.** 1993. Simian immunodeficiency virus RNA is efficiently encapsidated by human immunodeficiency virus type 1 particles. J. Virol. **67:**2681–2688.
43. **Sagata, N., T. Yasunaga, J. Tsuzuku-Kawamura, K. Ohishi, and Y. Ogawa.** 1985. Complete nucleotide sequence of the genome of bovine leukemia virus: its evolutionary relationship to other retroviruses. Proc. Natl. Acad. Sci. USA **82:**677–681.
44. **Sambrook, J., E. F. Fritsch, and T. Maniatis.** 1989. Molecular cloning: a laboratory manual, 2nd ed. Cold Spring Harbor Laboratory Press, Cold Spring Harbor, N.Y.
45. **Sorge, J., W. Ricci, and S. H. Hughes.** 1983. *cis*-acting RNA packaging locus

in the 115-nucleotide direct repeat of Rous sarcoma virus. J. Virol. **48:**667–675.
46. **Sundquist, W., and S. Heaphy.** 1993. Evidence for interstrand quadruplex formation in the dimerization of human immunodeficiency virus 1 genomic RNA. Proc. Natl. Acad. Sci. USA **90:**3393–3397.
47. **Temin, H. M.** 1968. Studies on carcinogenesis by avian sarcoma viruses. VIII. Glycolysis and cell multiplication. Int. J. Cancer **3:**273–282.
48. **Van der Maaten, M., and J. Miller.** 1976. Replication of bovine leukemia virus in monolayer cell cultures. Bibl. Haematol. **43:**360–362.
49. **Watanabe, S., and H. M. Temin.** 1982. Encapsidation sequences for spleen necrosis virus, an avian retrovirus, are between the 5′ long terminal repeat and the start of the gag gene. Proc. Natl. Acad. Sci. USA **79:**5986–5990.
50. **Weiss, R., N. Teich, H. Varmus, and J. Coffin.** 1985. RNA tumor viruses. Cold Spring Harbor Laboratory Press, Cold Spring Harbor, N.Y.
51. **Yang, S., and H. M. Temin.** 1994. A double hairpin structure is necessary for the efficient encapsidation of spleen necrosis virus retroviral RNA. EMBO J. **13:**713–726.
52. **Zuker, M.** 1989. On finding all suboptimal foldings of an RNA molecule. Science **244:**48–52.
53. **Zuker, M., and P. Stiegler.** 1981. Optimal computer folding of large RNA sequences using thermodynamics and auxiliary information. Nucleic Acids Res. **9:**133–148.